Inorganic Chemistry

Article

pubs.acs.org/IC

Molecular Iron(III) Phosphonates: Synthesis, Structure, Magnetism, and Mössbauer Studies

Joydeb Goura,[†] Prasenjit Bag,[†] Valeriu Mereacre,*[,‡] Annie K. Powell,[‡] and Vadapalli Chandrasekhar*[,†,§]

[†]Department of Chemistry, Indian Institute of Technology Kanpur, Kanpur 208016, India

[‡]Institute of Inorganic Chemistry, Karlsruhe Institute of Technology, Engesserstrasse 15, 76128 Karlsruhe, Germany

[§]National Institute of Science Education and Research, Institute of Physics Campus, Sachivalaya Marg, Sainik School, Bhubaneswar, Orissa 751 005, India

Supporting Information

ABSTRACT: The reaction of $Fe(ClO_4)_2·6H_2O$ with *t*-$BuPO_3H_2$ or $Cl_3CPO_3H_2$ in the presence of an ancillary pyrazole phenolate as a coligand, H_2phpzH [H_2phpzH = 3(5)-(2-hydroxyphenyl)pyrazole], afforded tetra- and pentanuclear Fe(III) phosphonate complexes $[Fe_4(t\text{-}BuPO_3)_4(HphpzH)_4]·5CH_3CN·5CH_2Cl_2$ (**1**) and $[HNEt_3]_2[Fe_5(\mu_3\text{-}O)(\mu\text{-}OH)_2(Cl_3CPO_3)_3(HphpzH)_5(\mu\text{-}phpzH]·3CH_3CN·2H_2O$ (**2**). Single-crystal X-ray structural analysis reveals that **1** possesses a cubic double-4-ring (D4R) core similar to what is found in zeolites. The molecular structure of **2** reveals it to be pentanuclear. It crystallizes in the chiral *P*1 space group. Magnetic studies on **1** and **2** have also been carried out, which reveal that the bridging phosphonate ligands mediate weak antiferromagnetic interactions between the Fe(III) ions. Magnetization dynamics of **1** and **2** have been corroborated by a Mössbauer spectroscopy analysis.

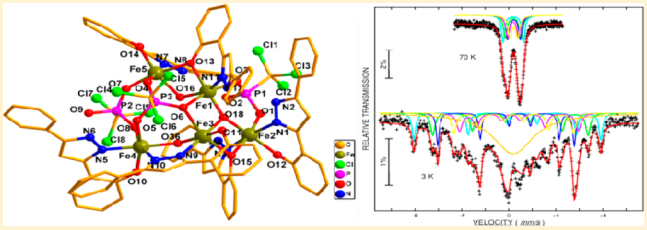

INTRODUCTION

The deprotonation of an organophosphonic acid $RP(O)(OH)_2$ with a base leads to the formation of organophosphonates $[RP(O)_2OH]^-$ and $[RPO_3]^{2-}$, which are excellent multidentate coordination ligands possessing binding capabilities that exceed those of other oxygen-containing ligands such as carboxylates.[1] Thus, an $[RPO_3]^{2-}$ ligand can in principle bind to a maximum of nine metal ions (Scheme 1).[1] However, this propensity to bind multiple metal ions can also be the undoing of this family of ligands, particularly with regard to isolation of molecular complexes.[1] In general, interaction of phosphonate ligands with transition metal ions leads, expectedly, to the formation of compounds possessing extended structures.[2] Molecular metal phosphonates can be achieved, however, by using two synthetic strategies. One of these consists of using an ancillary ligand that binds to the transition metal ion and restricts the number of available coordination sites and thereby reduces the chances of extended structures while simultaneously favoring molecular compounds.[3] The other strategy is the use of sterically hindered phosphonates, which prevent the formation of compounds possessing extended structures.[4] Using these two strategies and a combination of them we and others have been able to prepare and structurally characterize molecular transition metal phosphonates of varying nuclearities.[3,4] The most well-studied examples in this family contain Cu(II),[3−5] although recently other transition metal ions are also being tried for this purpose.[6,7] Surprisingly, Fe(III)- containing molecular phosphonates are considerably sparse. Most of these contain ancillary oxygen ligands such as carboxylates. Recently Dunbar and co-workers have reported an unprecedented Fe_{36} phosphonate cage without using any other ligands.[8] However, the phosphonate used in this case has a pyridyl nitrogen, which helps to fulfill the coordination sites of the iron centers.[8] Among low-nuclearity Fe(III) phosphonates pentanuclear derivatives are completely unknown, while in tetranuclear derivatives novel geometries resembling the D4R ring of zeolites are also unknown.[4a,5b,9] Herein, we report the synthesis and structure of carboxylate-free Fe(III) molecular phosphonates $[Fe^{III}_4(t\text{-}BuPO_3)_4(HphpzH)_4]·5CH_3CN·5CH_2Cl_2$ (**1**) and $[HNEt_3]_2[Fe^{III}_5(\mu_3\text{-}O)(\mu\text{-}OH)_2(Cl_3CPO_3)_3(HphpzH)_5(\mu\text{-}phpzH)]·3CH_3CN·2H_2O$ (**2**) [H_2phpzH = 3(5)-(2-hydroxyphenyl)pyrazole]. Detailed magnetic and Mössbauer studies are also reported.

Scheme 1. Possible Coordination Capability of a $[RPO_3]^{2-}$ Ligand

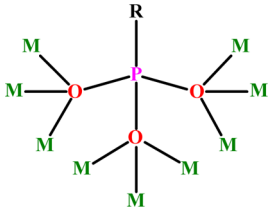

Received: May 24, 2014
Published: July 21, 2014

   dx.doi.org/10.1021/ic5012154 | *Inorg. Chem.* 2014, 53, 8147−8154

Scheme 2. Fe_3O Core-Containing Fe_4, Fe_6, Fe_7, Fe_8, and Fe_9 Phosphonates

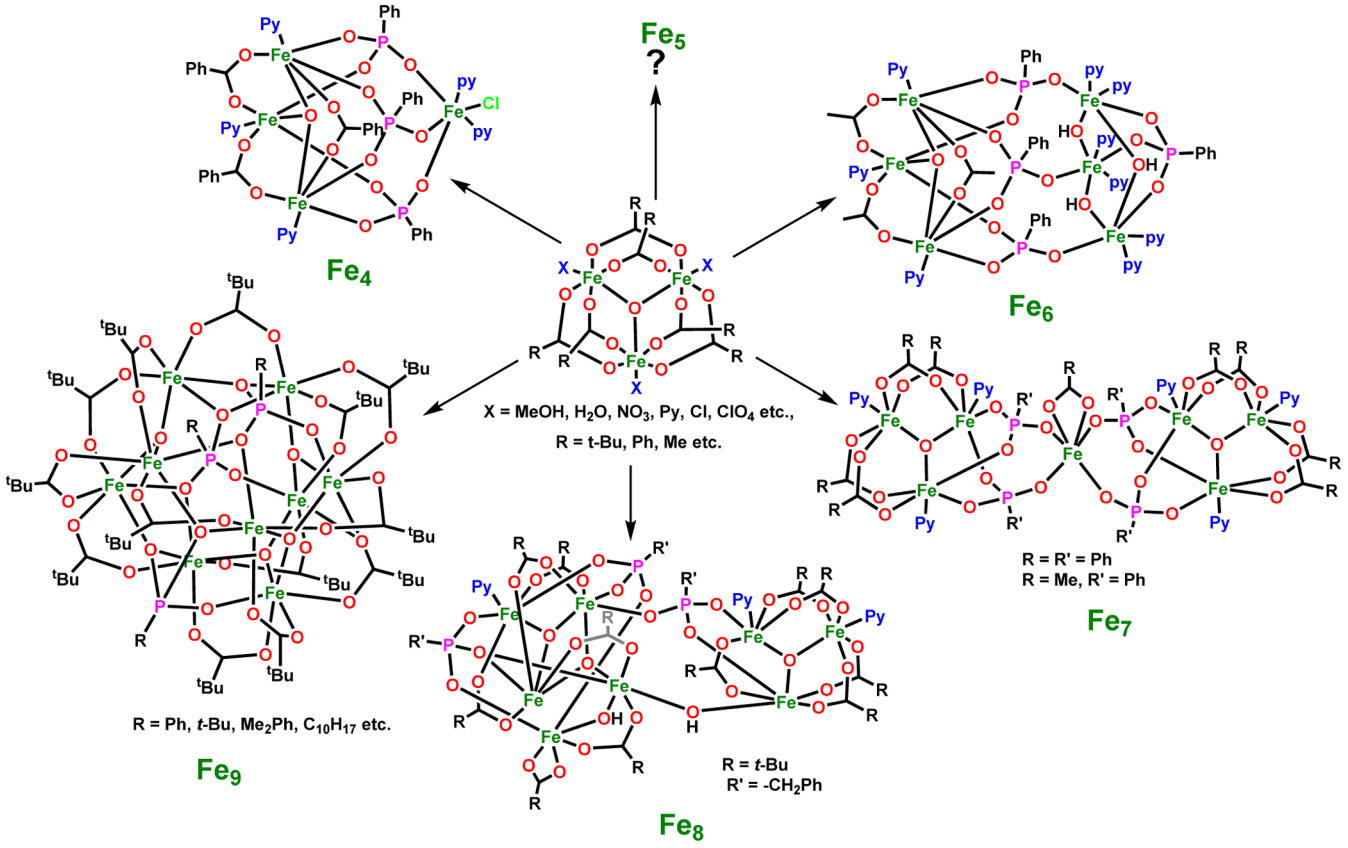

EXPERIMENTAL SECTION

Reagents and General Procedures. Solvents and other general reagents used in this work were purified according to standard procedures.[10] $Fe(ClO_4)_2{\cdot}6H_2O$, 1-(2-hydroxyphenyl)-3-phenyl-1,3-propanedione (Aldrich, USA), $AlCl_3$, PCl_3, CCl_4, and hydrazine hydrate ($N_2H_4{\cdot}H_2O$) (S. D. Fine Chemicals, India) were used as received. The phosphonic acids *t*-$BuPO_3H_2$,[11a] $Cl_3CPO_3H_2$,[11b] and 3(5)-(2-hydroxyphenyl)pyrazole [H_2phpzH][11c] were prepared according to the literature procedures.

Instrumentation. Melting points were measured using a JSGW melting point apparatus and are uncorrected. ^{1}H NMR spectra were recorded in $CDCl_3$ solutions on a JEOL JNM LAMBDA 400 model spectrometer operating at 400.0 MHz; chemical shifts are reported in parts per million (ppm) and are referenced with respect to internal tetramethylsilane. IR spectra were recorded as KBr pellets on a Bruker Vector 22 FT IR spectrophotometer operating at 400−4000 cm^{-1}. Elemental analyses of the compounds were obtained from Thermoquest CE Instruments model CHNS-O, EA/110. ESI-MS spectra were recorded on a Micromass QUATTRO II triple quadrupole mass spectrometer.

Magnetic Measurements. The magnetic susceptibility measurements were collected with the use of a Quantum Design MPMS-XL SQUID magnetometer. This magnetometer works between 1.8 and 400 K for dc applied fields ranging from −7 to 7 T. Measurements were carried out on finely ground polycrystalline samples. Alternating current susceptibility measurements were measured with an oscillating ac field of 3 Oe and ac frequencies ranging from 1 to 1500 Hz. The magnetic data were corrected for the sample holder.

The susceptibility data of complex **1** were analyzed on the basis of the usual spin-Hamiltonian description for the electronic ground state by using the simulation package *julX* written by Eckhard Bill.[12] The Hamilton operator is $\hat{H} = -2J_{ij}\hat{S}_i\hat{S}_j + g\beta\,\vec{S}\vec{B}$.

Mössbauer Spectroscopy. The Mössbauer spectra were acquired by using a conventional spectrometer in the constant-acceleration mode equipped with a ^{57}Co source (3.7 GBq) in a rhodium matrix. Isomer shifts are given relative to α-Fe at room temperature. The sample was inserted inside an Oxford Instruments Mössbauer-Spectromag 4000 cryostat, which has a split-pair superconducting magnet system for applied fields up to 6 T, with the field of the sample oriented perpendicular to the γ-ray direction, while the sample temperature can be varied between 3.0 and 300 K.

Synthesis. *[Fe^{III}_4(t-$BuPO_3$)$_4$(HphpzH)$_4$]·5CH_3CN·5CH_2Cl_2 (**1**).* $Fe(ClO_4)_2{\cdot}6H_2O$ (0.174 g, 0.480 mmol) was taken in acetonitrile (15 mL). To this was added a solution of 3(5)-(2-hydroxyphenyl)pyrazole (H_2phpzH) (0.113 g, 0.480 mmol) and *tert*-butylphosphonic acid (*t*-$BuPO_3H_2$) (0.033 g, 0.240 mmol) in dichloromethane (15 mL), and the resulting solution was stirred at room temperature for 6 h. At this stage, triethylamine (0.073 g, 0.721 mmol) was added to the reaction mixture. The resulting clear brown solution was stirred for an additional 12 h. The solution was evaporated, and the residue obtained was redissolved in DCM/MeCN (1:1) and filtered. The solution was left for slow evaporation at room temperature. After 15 days, brown block-shaped crystals of **1** were obtained. Yield: 0.166 g, 59% (based on Fe). Anal. Calcd for $C_{91}H_{105}Cl_{10}Fe_4N_{13}O_{16}P_4$ (2338.69) (**1**): C, 46.73; H, 4.53; N, 7.79. Found: C, 46.42; H, 4.29; N, 7.49. IR (KBr, ν, cm^{-1}): 3289(br), 3064(w), 2949(m), 1599(s), 1559(s), 1506(m), 1479(s), 1457(s), 1408(w), 1308(s), 1256(w), 1131(s), 1112(s), 1059(m), 1036(w), 1002(s), 984(s), 868(s), 831(w), 799(w), 753(s), 686(s), 661(s), 635(w), 567(s), 501(s), 419(s). ESI-MS: *m/z* 762.2018, [Fe(HphpzH)(^{t}$BuPO_3H$)$_3$ + Na + H + 2H_2O]$^+$; 899.5436, [Fe_2(HphpzH)(phpzH)(^{t}$BuPO_3$)$_2$ + 2Na]$^+$.

*[$HNEt_3$]$_2$[Fe^{III}_5(μ_3-O)(μ-OH)$_2$(Cl_3CPO_3)$_3$(HphpzH)$_5$(μ-phpzH)]·3CH_3CN·2H_2O (**2**).* $Fe(ClO_4)_2{\cdot}6H_2O$ (0.174 g, 0.480 mmol) was taken in methanol (15 mL). To this was added a solution of 3(5)-(2-hydroxyphenyl)pyrazole (H_2phpzH) (0.113 g, 0.480 mmol) and trichloromethyl phosphonic acid ($Cl_3CPO_3H_2$) (0.048 g, 0.240 mmol) in dichloromethane (15 mL), and the solution was stirred at room temperature for 6 h. At this stage, triethylamine (0.073 g, 0.721 mmol) was added to the reaction mixture. The resulting clear brown solution was stirred for an additional 12 h. The solution was evaporated, and

dx.doi.org/10.1021/ic5012154 | Inorg. Chem. 2014, 53, 8147−8154

the residue obtained was redissolved in DCM/MeCN (1:1) and filtered. The solution was left for slow evaporation at room temperature. After 10 days, brown block-shaped crystals of **2** were obtained. Yield: 0.146 g, 56% (based on Fe). Anal. Calcd for $C_{111}H_{112}Cl_9Fe_5N_{17}O_{20}P_3$ (2695.40) (**2**): C, 51.62; H, 4.26; N, 9.08. Found: C, 51.36; H, 4.06; N, 8.86. IR (KBr, ν, cm^{-1}): 3371(s), 2925(br), 1601(s), 1557(s), 1489(s), 1471(s), 1457(s), 1308(m), 1266(w), 1151(s), 1118(s), 1052(m), 1032(m), 1009(s), 984(s), 858(s), 757(s), 687(s), 659(w), 558(s), 507(s). ESI-MS: m/z 1487.1862, $[Fe_3(O)(HphpzH)_3(Cl_3CPO_3)_3 + Na + 4CH_3OH + 3H_2O]^+$.

X-ray Crystallography. Single-crystal X-ray structural studies of **1** and **2** were performed on a CCD Bruker SMART APEX diffractometer equipped with an Oxford Instruments low-temperature attachment. Data were collected using graphite-monochromated Mo Kα radiation (λ_α = 0.71073 Å). The crystals did not degrade/decompose during data collection. Data collection, structure solution, and refinement were performed using SMART, SAINT, and SHELXTL programs, respectively.[13a−f] All the calculations for the data reduction were done using the Bruker SADABS program. All the non-hydrogen atoms were refined anisotropically using full-matrix least-squares procedures. All the hydrogen atoms were included in idealized positions, and a riding model was used. The lattice solvent molecules (for complex **1**, $5CH_3CN$ and $5CH_2Cl_2$) could not be modeled satisfactorily due to the presence of heavy disorder. Therefore, the PLATON/"SQUEEZE"[13g,h] program was used to remove those disordered solvent molecules. The total electron count removed by SQEEZE corresponded to 640 (for complex **1**) per unit cell. This corresponds to 320 electrons per molecule (Z = 2) and is assigned to $5CH_3CN$ and $5CH_2Cl_2$ molecules for complex **1**. All the mean plane analyses as well as molecular drawings were obtained from DIAMOND (version 3.1).

RESULTS AND DISCUSSION

Synthesis. The preparation of polynuclear molecular Fe(III) phosphonate clusters was achieved earlier by various methods. Using the preformed trinuclear complex $[Fe_3(\mu_3\text{-}O)(RCO_2)_6(L)_3]X$ (R = Me, Ph, *t*-Bu; X = Cl, NO_3) as a starting material, by a cluster expansion strategy involving the replacement of labile ligands by phosphonates, multinuclear Fe(III) phosphonates that also contain carboxylate coligands have been prepared.[13] All such Fe(III)-phosphonates, known thus far, possess an Fe_3O core.[14] Representative examples are shown in Scheme 2.[14] Only four examples that do not contain an Fe_3O core are known: $[\{Fe_{36}L_{44}(H_2O)_{48}\}](ClO_4)_{2.1}(NO_3)_{11.9}(OH)_6{\cdot}47.9H_2O{\cdot}10EtOH$ (L = 2-$PyPO_3H$),[8] $[Fe_4(2\text{-}PyHCH_2PO_3)_4(H_2O)_{12}(Cl)(ClO_4)_7{\cdot}xH_2O]$,[15] $[Fe^{III}_4K_2(O_3P\text{-}t\text{-}Bu)_2(acac)_{10}]$,[16] and $[Fe_8Na_2(HL)_2(H_2L)_{10}(H_2O)_6]{\cdot}22H_2O$.[17] Recently, we have utilized chelating nitrogen ligands [(1,10-phenanthroline (phen) or 2,6-bis(pyrazol-3-yl)pyridine (dPzPy)] in conjunction with organophosphonic acids and Mn(II) salts and were able to modulate the nuclearity of the resulting assemblies from 2 to 4.[18] We wished to explore if such a strategy could also be applied to the synthesis of Fe(III) phosphonates. Accordingly, the reaction of $Fe(ClO_4)_2{\cdot}6H_2O$ with *tert*-butylphosphonic acid (*t*-$BuPO_3H_2$) or trichloromethylphosphonic acid ($Cl_3CPO_3H_2$) in the presence of the chelating nitrogen ligand 3(5)-(2-hydroxyphenyl)pyrazole [H_2phpzH] was carried out, affording tetra- and pentanuclear derivatives $[Fe_4(t\text{-}BuPO_3)_4(HphpzH)_4]{\cdot}5CH_3CN{\cdot}5CH_2Cl_2$ (**1**) and $[HNEt_3]_2[Fe_5(\mu_3\text{-}O)(\mu\text{-}OH)_2(Cl_3CPO_3)_3(HphpzH)_5(\mu\text{-}phpzH)]{\cdot}3CH_3CN{\cdot}2H_2O$ (**2**). The molecular structures of compounds **1** and **2** were determined by single-crystal X-ray crystallography (vide infra). ESI-MS of **1** and **2** reveals the fragmentation of these complexes in solution (see the Experimental Section and the Supporting Information). Thus, the ESI-MS of **2** reveals the presence of a trinuclear motif (m/z = 1487.1862), $[Fe_3(O)(HphpzH)_3(Cl_3CPO_3)_3 + Na + 4CH_3OH + 3H_2O]^+$ (Figure 1).

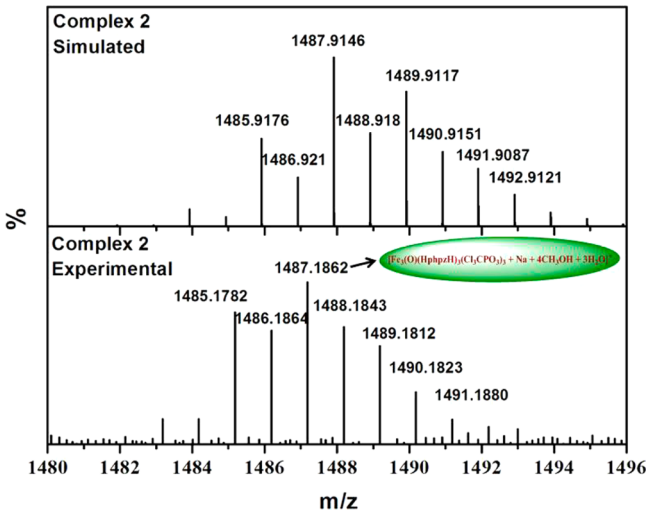

Figure 1. ESI-MS spectra of **2**: experimental (bottom) and simulated (top).

Molecular Structures of 1 and 2. The molecular structures of **1** and **2** were determined by X-ray crystallography. The crystallographic parameters of these compounds are given in Table 1. The various coordination modes of the phosphonate and phosphinate ligands observed in **1** and **2** are summarized in Scheme 3. Compound **1** crystallized in the triclinic system ($P\bar{1}$). On the other hand **2** crystallized in the chiral space group $P1$. The refined Flack parameter of **2** is 0.018(14), which indicates the crystallization of enantiopure forms. However, for the bulk sample, circular dichroism experiments did not show any signal. This is probably due to the presence of a conglomerate (racemic mixture of crystals of the two enantiomers that crystallize out separately).[19]

The molecular structure of **1** reveals that it is a cubic tetramer with a double-4-ring (D4R) core, reminiscent of secondary building units found in zeolites (Scheme 4 and Figure 2). Iron and phosphorus atoms occupy alternate vertices of a distorted cube. The edges of the cube contain oxygen atoms. Four $[t\text{-}BuPO_3]^{2-}$ ligands assist the formation of the D4R tetramer; each phosphonate binds to three iron centers through a 3.111 coordination mode (Harris notation; see Scheme 3).[20] The three P−O bond distances involved are P(1)−O(4) 1.519(3) Å, P(1)−O(2) 1.523(3) Å, and P(1)−O(3) 1.543(4) Å. The Fe−O distances found in the complex are also very similar: Fe(1)−O(2) 1.900(3) Å, Fe(1)−O(3) 1.945(3) Å, and Fe(1)−O(4) 1.956(3) Å. The other important bond parameters of this compound are given in Table 2. In addition to the phosphonate ligands each of the iron centers is also bound with a $N\wedge O$ chelating $[HphpzH]^-$. The corresponding Fe−O and Fe−N bond distances are Fe(1)−O(1) 1.856(3) Å and Fe(1)−N(1) 2.093(4) Å. Each Fe(III) center in **1** is, thus, five-coordinate (1N, 4O) and is present in a distorted square-pyramidal configuration (Figure 2c and Supporting Information). The molecular structure of **1** is grossly similar to some transition metal/main-group metal phosphonates that have previously been shown to possess D4R cores.[4a,5b,9]

Compound **2** is a dianionic pentanuclear complex (Scheme 5 and Figure 3). The Fe−O−P core of **2** is shown in Figure 3b. A

dx.doi.org/10.1021/ic5012154 | Inorg. Chem. 2014, 53, 8147−8154

Table 1. Crystal Data and Structure Refinement Parameters of 1 and 2

	1	2
formula	$C_{76}H_{80}Fe_4N_8O_{16}P_4$	$C_{111}H_{108}Cl_9Fe_5N_{17}O_{20}P_3$
fw	1708.76	2691.36
temp (K)	100(2)	100(2)
cryst syst	tetragonal	triclinic
space group	$P4_2/n$	$P1$
a (Å)	21.070(5)	13.793(5)
b (Å)	21.070(5)	16.125(5)
c (Å)	10.811(5)	16.939(5)
α (deg)	90	105.022(5)
β (deg)	90	106.930(5)
γ (deg)	90	112.167(5)
volume (Å^3); Z	4799(3); 2	3034.4(17); 1
density (Mg m^{-3})	1.182	1.473
abs coeff (mm^{-1})	0.717	0.893
F(000)	1768	1381
cryst size (mm)	0.28 × 0.26 × 0.24	0.18 × 0.16 × 0.14
θ range (deg)	4.10 to 25.02	4.12 to 25.03
limiting indices	$-25 \le h \le 20$; $-24 \le k \le 25$; $-12 \le l \le 12$	$-15 \le h \le 16$; $-19 \le k \le 17$; $-19 \le l \le 20$
reflns collected	24 112	20 904
unique reflns [R_{int}]	4218 [0.0513]	14 389 [0.0305]
completenes to θ	99.5% (25.02°)	99.3% (25.03°)
data/restraints/params	4218/12/251	14389/29/1477
GOOF on F^2	1.063	1.032
final R indices [$I > 2\sigma(I)$]	R_1 = 0.0699, wR_2 = 0.1756	R_1 = 0.0501, wR_2 = 0.1231
R indices (all data)	R_1 = 0.0838, wR_2 = 0.1821	R_1 = 0.0605, wR_2 = 0.1290
absolute struct param		0.018(14)
largest residual peaks (e Å^{-3})	0.772 and −0.515	1.950 and −1.950

Scheme 3. Coordination Modes of $[RPO_3]^{2-}$, $HphpzH^-$, $phpzH^{2-}$, O^{2-}, and OH^- Ligands as Observed in the Present Study[a]

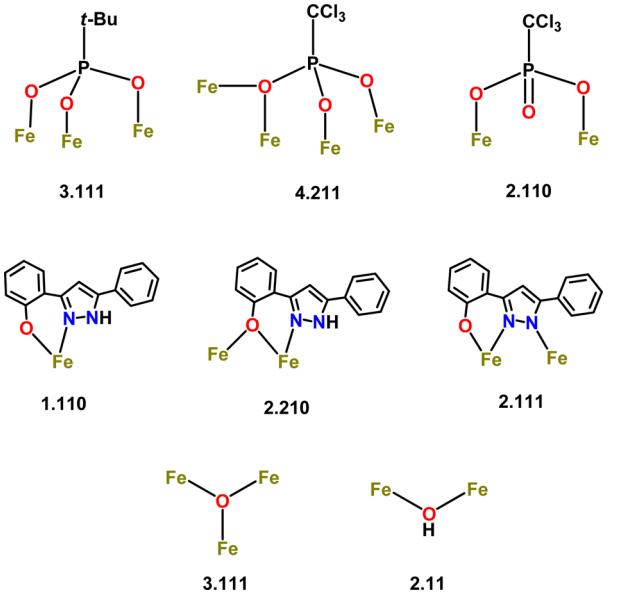

[a]R = *t*-Bu, Cl_3C.

Scheme 4. Synthesis of 1

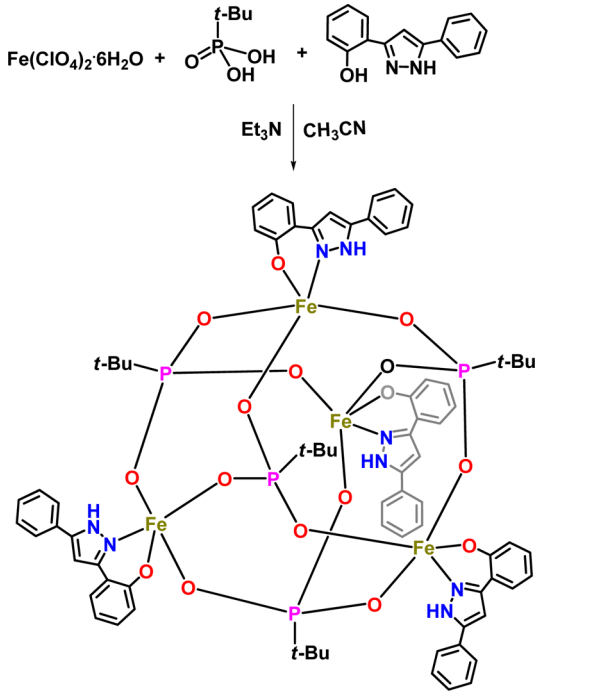

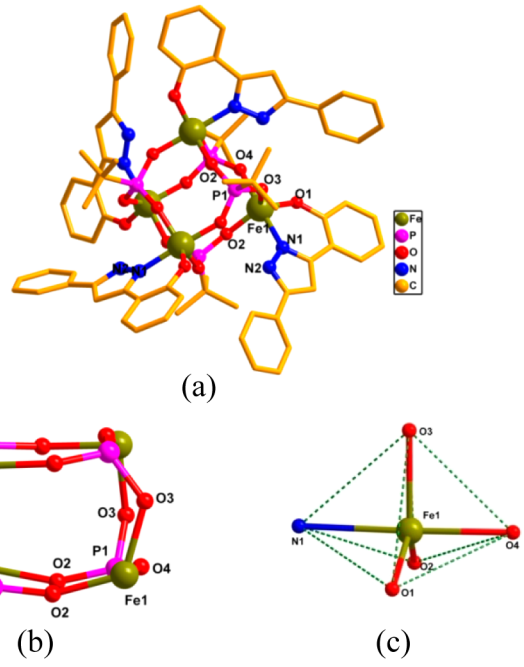

Figure 2. (a) Molecular structure of **1**. All the hydrogen atoms have been omitted for clarity. (b) Fe–O–P core of **1**. (c) Distorted square-pyramidal geometry of the Fe center in **1** (τ = 0.88).[22]

major difference in the structures of **1** and **2** arises from the bridging coordination action of the ancillary ligand. Both the phenolate oxygen and the pyrazolyl nitrogen contribute to the bridging coordination. In addition, each iron center is bound by the chelating coordination action of the ancillary ligand (N^O). Within the pentanuclear core three iron centers (Fe1, Fe2, Fe3) are held together by a 3.111 (μ_3-O) mode. On the other hand, Fe1 and Fe5 as well as Fe3 and Fe4 are held together by a 2.11 (μ-OH) mode. Overall, three phosphonate ligands are involved in the complex formation. One of these binds in a 4.211 mode

dx.doi.org/10.1021/ic5012154 | Inorg. Chem. 2014, 53, 8147–8154

Table 2. Important Bond Lengths and Bond Angles of Compound 1

bond lengths (Å)	bond lengths (Å)	bond angles (deg)
Fe(1)–O(1) 1.856(3)	P(1)–O(4) 1.519(3)	O(1)–Fe(1)–O(2) 124.26(15)
Fe(1)–O(2) 1.900(3)	P(1)–O(2) 1.523(3)	O(1)–Fe(1)–O(3) 113.87(15)
Fe(1)–O(3) 1.945(3)	P(1)–O(3) 1.543(4)	O(2)–Fe(1)–O(3) 121.31(14)
Fe(1)–O(4) 1.956(3)		O(1)–Fe(1)–O(4) 94.29(15)
Fe(1)–N(1) 2.093(4)		O(2)–Fe(1)–O(4) 93.40(13)
		O(3)–Fe(1)–O(4) 89.65(14)

Scheme 5. Synthesis of 2

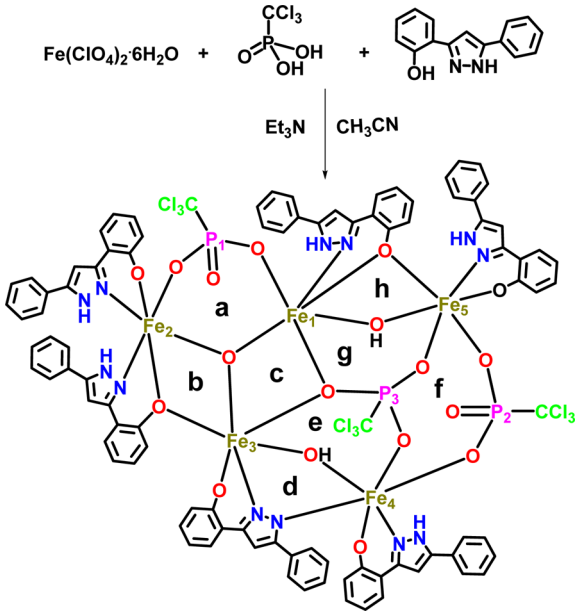

and binds Fe1, Fe3, Fe4, and Fe5. The other two phosphonates bind in a 2.110 mode (Scheme 5 and Figure 3). Fe2, Fe4, and Fe5 possess an exclusive chelating 3(5)-(2-hydroxyphenyl)-pyrazole (H_2phpzH). Finally, the periphery of the pentanuclear core is stitched together by the chelating coordination action of the ancillary ligand; while Fe2 and Fe3 (similarly Fe1 and Fe5) are connected by a bridging phenolate oxygen, Fe3 and Fe4 are bridged by the 2.11 (η^1, η^1) coordination of the pyrazole motif. The binding nature of the hydroxide [HO^-] and oxide [O^{2-}] were confirmed by the bond valence sum calculations (Supporting Information).[21] The important bond parameters of this compound are given in Table 3. Interestingly, eight metallacycles of varied sizes are generated within the pentanuclear core assembly (Scheme 5, Figure 3b). The coordination environment around the Fe(III) centers is either (5O,N) or (4O,2N); the coordination geometry is distorted octahedral (Figure 3c and d).

Magnetic Studies. The magnetic susceptibility of compound **1** was measured in the range 1.8–300 K under a constant magnetic field of 0.1 T (Figure 4). At room temperature, the χT product is 15.7 cm^3 mol^{-1} K, below the 17.5 cm^3 mol^{-1} K value that is expected for a tetranuclear species containing four noninteracting high-spin Fe(III) centers (S = 5/2 and g = 2). When the temperature is lowered, the χT

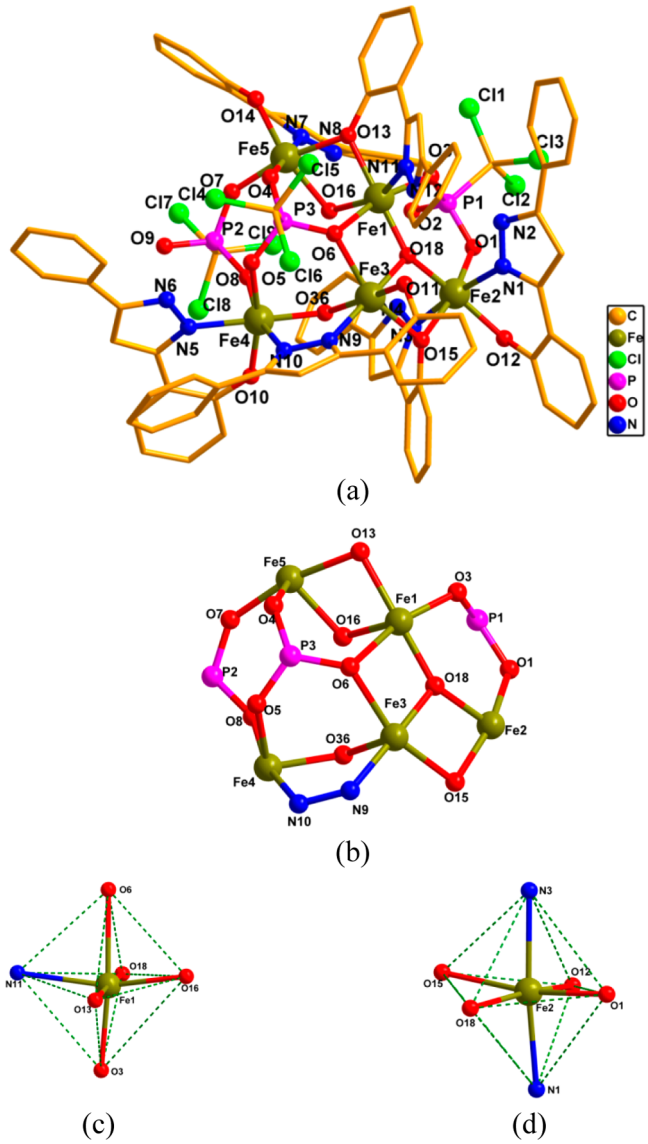

Figure 3. (a) Molecular structure of **2**. All the hydrogen atoms have been omitted for clarity. (b) Fe–O–P core of **2**. (c and d) Distorted octahedral geometry of the Fe center in **2**.

product decreases continuously to reach a value close to zero at 1.8 K. These data characterize an antiferromagnetic exchange interaction between the metal centers, leading to an S = 0 ground state. The shape of the magnetization and its value at measured temperatures also support this conclusion. Inspection of the molecular structure of **1** highlights the presence of one type of coupling constant, which describes the exchange coupling through the PO_3 bridging groups. If we neglect zero-field splitting of the high-spin Fe(III) sites, the best fit leads to J = −2.47(1) cm^{-1} assuming g = 2.00 (Figure 4). These values fit very well with the observed temperature-dependence shape and room-temperature χT values and indicate very weak antiferromagnetic interaction between the iron centers.

The χT value at 300 K for complex **2** (12.34 cm^3 mol^{-1} K) is well below the theoretically expected value of five noninteracting S = 5/2 spins (21.88 cm^3 mol^{-1} K), indicating large antiferromagnetic interactions (Figure 5). This is corroborated by the decrease of χT upon cooling, reaching a value around 7 K (4.34 cm^3 mol^{-1} K), indicative of an S = 5/2

dx.doi.org/10.1021/ic5012154 | Inorg. Chem. 2014, 53, 8147–8154

Table 3. Important Bond Lengths and Bond Angles of Compound 2

bond lengths (Å)	bond lengths (Å)	bond lengths (Å)	bond angles (deg)
Fe(1)–O(18) 1.866(5)	Fe(3)–N(9) 2.050(6)	P(1)–O(2) 1.492(5)	Fe(1)–O(18)–Fe(2) 142.8(3)
Fe(1)–O(16) 1.963(4)	Fe(3)–O(6) 2.125(5)	P(1)–O(1) 1.520(5)	Fe(1)–O(18)–Fe(3) 110.4(2)
Fe(1)–O(3) 1.979(5)	Fe(4)–O(10) 1.898(5)	P(1)–O(3) 1.524(5)	Fe(2)–O(18)–Fe(3) 105.5(2)
Fe(1)–O(13) 2.030(5)	Fe(4)–O(36) 1.962(5)	P(2)–O(9) 1.499(5)	Fe(1)–O(16)–Fe(5) 103.9(2)
Fe(1)–O(6) 2.206(5)	Fe(4)–O(8) 2.005(5)	P(2)–O(8) 1.510(5)	Fe(1)–O(16)–Fe(5) 103.9(2)
Fe(2)–O(18) 1.914(5)	Fe(4)–O(5) 2.043(5)	P(2)–O(7) 1.520(5)	Fe(4)–O(36)–Fe(3) 122.0(2)
Fe(2)–O(12) 1.967(5)	Fe(5)–O(14) 1.910(5)	P(3)–O(4) 1.498(5)	Fe(4)–O(36)–Fe(3) 122.0(2)
Fe(2)–O(1) 1.986(5)	Fe(5)–O(7) 1.964(5)	P(3)–O(5) 1.516(5)	
Fe(2)–O(15) 2.044(5)	Fe(5)–O(16) 2.008(5)	P(3)–O(6) 1.534(5)	
Fe(3)–O(11) 1.948(5)	Fe(5)–O(4) 2.053(5)		
Fe(3)–O(18) 1.950(5)	Fe(5)–O(13) 2.083(4)		
Fe(3)–O(36) 1.992(4)	Fe(5)–N(7) 2.116(6)		
Fe(3)–O(15) 2.039(5)			

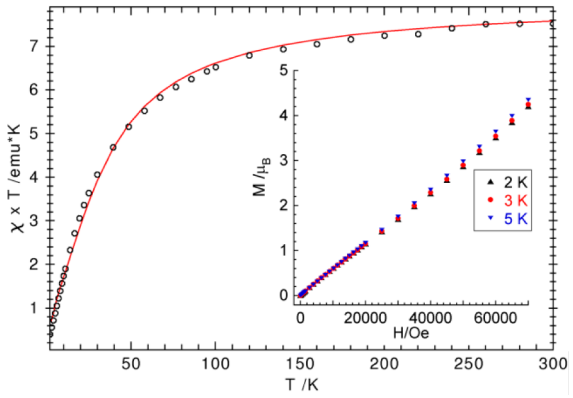

Figure 4. Temperature dependence of the susceptibility data, plotted as χT vs T considered for two iron centers of **1**. The solid line represents the results of best fitting. Inset: Magnetization data at 2, 3, and 5 K.

ground state (4.37 cm^3 mol^{-1} K). It shows a weakly defined plateau below 10 K. The lack of a clear plateau suggests the presence of low-lying excited states.

The magnetization studies at 2, 3, and 5 K for complex **2** revealed no saturation even at 70 kOe, but very close to being saturated with magnetization values of 5.00 μ_B, corresponding to $S = 5/2$ ground states (Figure 5). This is in agreement with the variable-temperature experiments, which revealed the presence of a weakly defined low-temperature χT plateau, at a value consistent with an ideal $S = 5/2$ spin ($g = 2$). However, the simulations of both dependencies were not successful, possibly due to complexities arising from the presence of low-lying excited states. Hence, variable field and temperature magnetization experiments confirm the $S = 5/2$ ground spin state value that was suggested on the basis of variable-temperature dc magnetic susceptibility measurements and

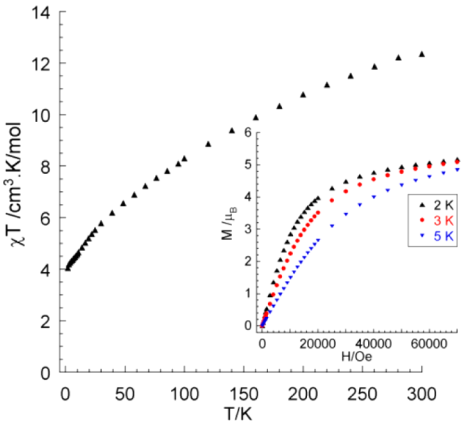

Figure 5. Temperature dependence of the susceptibility data, plotted as χT vs T at 0.1 T, for compound **2** and (inset) magnetization data at 2, 3, and 5 K.

expected for such a geometrical arrangement of five Fe^{III} high-spin centers.

Mössbauer Studies. The Mössbauer spectrum of **1** obtained at 3 K indicates the absence of any magnetic pattern and has been analyzed with one doublet with hyperfine parameters typically observed for Fe(III) high spin (Figure 6).

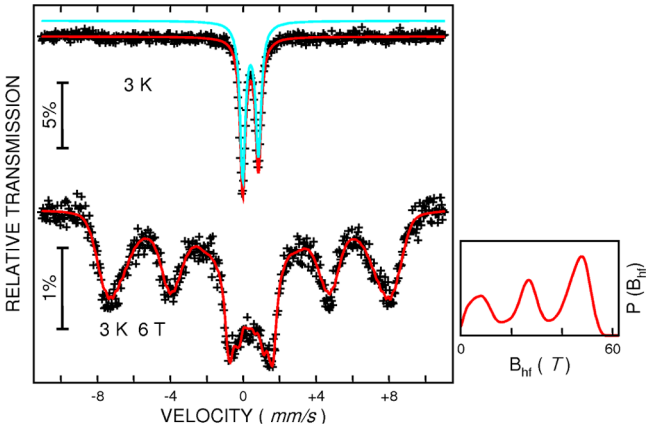

Figure 6. Mössbauer spectra for **1** at 3 K in zero-field and an applied field of 6 T.

This shows that the magnetic moments are not completely frozen, but still relax at a rate faster than the Mössbauer time scale. An additional aid for a complete frozen relaxation usually is an external magnetic field. The applied magnetic fields at low temperature will magnetize the net spin of the cluster along the field direction and decrease the relaxation time. The shape of the obtained magnetic spectra usually represents magnetic sextets. However, what we observe is completely different: when an external magnetic field of 6 T is applied, the obtained spectrum is dominated by intermediate relaxation phenomena with broad magnetic hyperfine lines superimposed on a sharp absorption envelope at the center of the spectrum. This result indicates that fast electronic relaxation can occur in these types of compounds even at liquid-helium temperatures and in a 6 T applied field. Higher fields are needed to freeze completely the magnetic moments.

The spectra for compound **2** at 70 K have been analyzed with the superposition of five symmetric Lorentzian doublets with very similar isomer shifts, but different quadrupole splittings

dx.doi.org/10.1021/ic5012154 | Inorg. Chem. 2014, 53, 8147–8154

assigned to the five crystallographically nonequivalent Fe(III) sites (Figure 7). This estimate is reasonable because the

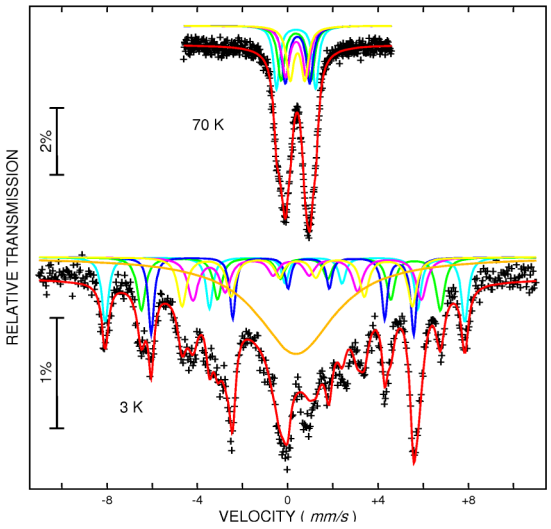

Figure 7. Mössbauer spectra for **2** at 70 and 3 K in zero-field.

Fe(1)−Fe(5) pseudooctahedral Fe(III) ions in **2** all have very similar valence and, thus, will exhibit rather similar isomer shifts, but the structure analysis reveals a range of bond length distortions for these Fe(III) environments that will lead to a range of quadrupole splittings. At lower temperatures than 70 K, the Mössbauer spectra are dominated by intermediate relaxation phenomena.

At 3 K (Figure 7), contrary to **1**, a well-defined magnetic spectrum (a superposition of several sextets, which confirm the presence of several crystallographically different iron centers and, respectively, different directions of the electronic spin density on every one) is obtained, indicating that the spin-relaxation has crossed from fast to slow with respect to the Mössbauer time scale. Although the fit of spectra in the paramagnetic region was successfully made by a superposition of five doublets, the best fit for the spectrum at 3 K was only achieved with five sextets and a very broad central pattern, which shows that at this temperature part of the iron centers are still relaxing with an intermediate relaxation time.

More information can be gained from the spectra measured at 3 K under applied fields. Applying strong external magnetic fields in combination with results obtained from paramagnetic spectra at higher temperatures, one can get information about the spin structure of the studied coordination clusters. We have also considered such experiments, but the spectra were too complex and broad to start with.

CONCLUSION

We were able to synthesize new tetra- and pentanuclear molecular iron phosphonate complexes in three-component reactions involving an Fe(II) salt, with phosphonic acids [*t*-$BuPO_3H_2$ or $Cl_3CPO_3H_2$] and chelating ancillary pyrazole ligands [H_2phpzH = 3(5)-(2-hydroxyphenyl)pyrazole]. We have shown that even without cluster expansion strategies we can isolate molecular Fe(III) phosphonate cages by direct reaction methods. In this paper, we report two novel molecular Fe(III) phosphonates cages, a tetranuclear Fe(III) phosphonate with a D4R core and a pentanuclaer Fe(III) phosphonate cage. These represent the first examples of their type in this family of compounds. Magnetic studies reveal that Fe(III)-phosphonate complexes display weak antiferromagnetic coupling mediated by the phosphonate ligands. The magnetization dynamics of complexes **1** and **2** have been corroborated by Mössbauer spectroscopy.

ASSOCIATED CONTENT

Supporting Information

Figures and tabulated bond angles/lengths for the crystal structures of compounds **1** and **2**. Mössbauer spectrum of compound **2** at 20 K. This material is available free of charge via the Internet at http://pubs.acs.org.

AUTHOR INFORMATION

Corresponding Authors

*E-mail: valeriu.mereacre@kit.edu.
*E-mail: vc@iitk.ac.in; vc@niser.ac.in.

Notes

The authors declare no competing financial interest.

ACKNOWLEDGMENTS

We thank the Department of Science and Technology, India, and the Council of Scientific and Industrial Research, India, for financial support. V.C. is thankful to the Department of Science and Technology, for a J. C. Bose fellowship. J.G. and P.B. thank the Council of Scientific and Industrial Research, India, for a Senior Research Fellowship. V.M. and A.K.P. acknowledge the DFG-funded transregional collaborative research center SFB/TRR 88 "3MET".

REFERENCES

(1) Chandrasekhar, V.; Senapati, T.; Dey, A.; Hossain, S. *Dalton Trans.* **2011**, *40*, 5394−5418.

(2) (a) Taylor, J. M.; Mah, R. K.; Moudrakovski, I. L.; Ratcliffe, C. I.; Vaidhyanathan, R.; Shimizu, G. K. H. *J. Am. Chem. Soc.* **2010**, *132*, 14055−14057. (b) Shimizu, G. K. H.; Vaidhyanathan, R.; Taylor, J. M. *Chem. Soc. Rev.* **2009**, *38*, 1430−1449. (c) Li, J.-T.; Keene, T. D.; Cao, D.-K.; Decurtins, S.; Zheng, L.-M. *CrystEngComm* **2009**, *11*, 1255−1260. (d) Taylor, J. M.; Mahmoudkhani, A. H.; Shimizu, G. K. H. *Angew. Chem., Int. Ed.* **2007**, *46*, 795−798. (e) Liang, J.; Shimizu, G. K. H. *Inorg. Chem.* **2007**, *46*, 10449−10451. (f) Bao, S. S.; Chen, G. S.; Wang, Y.; Li, Y. Z.; Zheng, L. M.; Luo, Q. H. *Inorg. Chem.* **2006**, *45*, 1124−1129. (g) Odobel, F.; Bujoli, B.; Massiot, D. *Chem. Mater.* **2001**, *13*, 163−173.

(3) (a) Chandrasekhar, V.; Kingsley, S. *Angew. Chem., Int. Ed.* **2000**, *39*, 2320−2322. (b) Brechin, E. K.; Coxall, R. A.; Parkin, A.; Parsons, S.; Tasker, P. A.; Winpenny, R. E. P. *Angew. Chem., Int. Ed.* **2001**, *40*, 2700−2703. (c) Langley, S.; Helliwell, M.; Raftery, J.; Tolis, E. I.; Winpenny, R. E. P. *Chem. Commun.* **2004**, 142−143. (d) Ali, S.; Baskar, V.; Muryn, C. A.; Winpenny, R. E. P. *Chem. Commun.* **2008**, 6375−6377. (e) Langley, S.; Helliwell, M.; Sessoli, R.; Teat, S. J.; Winpenny, R. E. P. *Dalton Trans.* **2009**, 3102−3110. (f) Zheng, Y.-Z.; Pineda, E. M.; Helliwell, M.; Winpenny, R. E. P. *Chem.—Eur. J.* **2012**, *18*, 4161−4165. (g) Zhang, L.; Clérac, R.; Heijboer, P.; Schmitt, W. *Angew. Chem., Int. Ed.* **2012**, *51*, 1−6. (h) Ma, Y. S.; Song, Y.; Li, Y. Z.; Zheng, L. M. *Inorg. Chem.* **2007**, *46*, 5459−5461. (i) Du, Z. Y.; Prosvirin, A. V.; Mao, J. G. *Inorg. Chem.* **2007**, *46*, 9884−9894. (j) Wang, M.; Ma, C. B.; Yuan, D. Q.; Wang, H. S.; Chen, C. N.; Liu, Q. T. *Inorg. Chem.* **2008**, *47*, 5580−5590.

(4) (a) Baskar, V.; Shanmugam, M.; Sañudo, E. C.; Collison, D.; McInnes, E. J. L.; Wei, Q.; Winpenny, R. E. P. *Chem. Commun.* **2007**, 37−39. (b) Teat, G. S.; Mallah, T.; Sessoli, R.; Wernsdorfer, W.; Winpenny, R. E. P. *Angew. Chem., Int. Ed.* **2005**, *44*, 5044−5048. (c) Chandrasekhar, V.; Sasikumar, P.; Boomishankar, R.; Anantharaman, G. *Inorg. Chem.* **2006**, *45*, 3344−3351. (d) Chan-

drasekhar, V.; Sasikumar, P.; Boomishankar, R. *Dalton Trans.* **2008**, 5189−5196. (e) Chandrasekhar, V.; Sasikumar, P.; Senapati, T.; Dey, A. *Inorg. Chim. Acta* **2010**, *363*, 2920−2928.

(5) (a) Chandrasekhar, V.; Senapati, T.; Clérac, R. *Eur. J. Inorg. Chem.* **2009**, 1640−1646. (b) Chandrasekhar, V.; Nagarajan, L.; Cleérac, R.; Ghosh, S.; Verma, S. *Inorg. Chem.* **2008**, *47*, 1067−1073. (c) Chandrasekhar, V.; Nagarajan, L. *Dalton Trans.* **2009**, 6712−6714. (d) Chandrasekhar, V.; Nagarajan, L.; Gopal, K.; Baskar, V.; Kögerler, P. *Dalton Trans.* **2005**, 3143−3145. (e) Chandrasekhar, V.; Senapati, T.; Dey, A.; Sañudo, E. C. *Inorg. Chem.* **2011**, *50*, 1420−1428. (f) Chandrasekhar, V.; Nagarajan, L.; Hossain, S.; Gopal, K.; Ghosh, S.; Verma, S. *Inorg. Chem.* **2012**, *51*, 5605−5616. (g) Chandrasekhar, V.; Senapati, T.; Sañudo, E. C.; Clérac, R. *Inorg. Chem.* **2009**, *48*, 6192−6204. (h) Chandrasekhar, V.; Kingsley, S.; Vij, A.; Lam, K. C.; Rheingold, A. L. *Inorg. Chem.* **2000**, *39*, 3238−3242. (i) Chandrasekhar, V.; Senapati, T.; Sañudo, E. C. *Inorg. Chem.* **2008**, *47*, 9553−9560. (j) Chandrasekhar, V.; Sahoo, D.; Narayanan, R. S.; Butcher, R. J.; Lloret, F.; Pardo, E. *Dalton Trans.* **2013**, *42*, 8192−8196.

(6) (a) Khanra, S.; Kloth, M.; Mansaray, H.; Muryn, C. A.; Tuna, F.; Sañudo, E. C.; Helliwell, M.; E. McInnes, J. L.; Winpenny, R. E. P. *Angew. Chem., Int. Ed.* **2007**, *46*, 5568−5571. (b) Salta, J.; Chen, Q.; Chang, Y.-D.; Zubieta, J. *Angew. Chem., Int. Ed.* **1994**, *33*, 757−760. (c) Salta, J.; Zubieta, J. *J. Cluster Sci.* **1997**, *8*, 361−380. (d) Dendrinou-Samara, C.; Muryn, C. A.; Tuna, F.; Winpenny, R. E. P. *Eur. J. Inorg. Chem.* **2010**, 3097−3101. (e) Shanmugam, M.; Shanmugam, M.; Chastanet, G.; Sessoli, R.; Mallah, T.; Wernsdorfer, W.; Winpenny, R. E. P. *J. Mater. Chem.* **2006**, *16*, 2576−2578. (f) Shanmugam, M.; Chastanet, G.; Mallah, T.; Sessoli, R.; Teat, S. J.; Timco, G. A.; Winpenny, R. E. P. *Chem.—Eur. J.* **2006**, *12*, 8777−8785. (g) Wang, M.; Ma, C.; Yuan, D.; Hu, M.; Chen, C.; Liua, Q. *New J. Chem.* **2007**, *31*, 2103−2110. (h) Wang, M.; Ma, C.; Chen, C. *Dalton Trans.* **2008**, 4612−4620.

(7) (a) Ma, K.-R.; Xu, J.-N.; Ning, D.-K.; Shi, J.; Zhang, D.-J.; Fan, Y.; Song, T.-Y. *Inorg. Chem. Commun.* **2009**, *12*, 119−121. (b) Breeze, B. A.; Shanmugam, M.; Tuna, F.; Winpenny, R. E. P. *Chem. Commun.* **2007**, 5185−5187. (c) Chandrasekhar, V.; Sahoo, D.; Metre, R. K. *CrystEngComm* **2013**, *15*, 7419−7422. (d) Langley, S.; Helliwell, M.; Sessoli, R.; Teat, S. J.; Winpenny, R. E. P. *Inorg. Chem.* **2008**, *47*, 497−507.

(8) Beavers, C. M.; Prosverin, A. V.; Cashion, J. D.; Dunbar, K. R.; Richards, A. F. *Inorg. Chem.* **2013**, *52*, 1670−1672.

(9) (a) Chandrasekhar, V.; Dey, A.; Senapati, T.; Sañudo, E. C. *Dalton Trans.* **2012**, *41*, 799−803. (b) Yang, Y.; Pinkas, J.; Schäfer, M.; Roesky, H. W. *Angew. Chem., Int. Ed.* **1998**, *37*, 2650−2653. (c) Yang, Y.; Schmidt, H.-G.; Noltemeyer, M.; Pinkas, J.; Roesky, H. W. *J. Chem. Soc., Dalton Trans.* **1996**, 3609−3610. (d) Walawalkar, M. G.; Murugavel, R.; Roesky, H. W.; Schmidt, H.-G. *Inorg. Chem.* **1997**, *36*, 4202−4207. (e) Mason, M. R.; Mashuta, M. S.; Richardson, J. F. *Angew. Chem., Int. Ed. Engl.* **1997**, *36*, 239−241. (f) Murugavel, R.; Shanmugan, S. *Dalton Trans.* **2008**, 5358−5367. (g) Walawalkar, M. G.; Murugavel, R.; Roesky, H. W.; Usón, I.; Kraetzner, R. *Inorg. Chem.* **1998**, *37*, 473−478.

(10) Vogel, A. I.; Furnis, B. S.; Hannaford, A. J.; Smith, P. W. G.; Tatchell, A. R. *Vogel's Textbook of Practical Organic Chemistry*, 5th ed.; Longman: London, 1989.

(11) (a) Crofts, P. C.; Kosolapoff, G. M. *J. Am. Chem. Soc.* **1953**, *75*, 3379−3383. (b) Bengelsdorf, I. S.; Barron, L. B. *J. Am. Chem. Soc.* **1955**, *77*, 2869−2871. (c) Addison, A. W.; Burke, P. J. *J. Heterocycl. Chem.* **1981**, *18*, 803−805.

(12) Bill, E. *julX Magnetic Analysis Program*; http://www.mpibac.mpg.de/bac/logins/bill/julX_en.php.

(13) (a) *SMART* and *SAINT* Software Reference manuals, Version 6.45; Bruker Analytical X-ray Systems, Inc.: Madison, WI, 2003. (b) Sheldrick, G. M. *SADABS*, software for empirical absorption correction, Ver. 2.05; University of Göttingen: Göttingen, Germany, 2002. (c) *SHELXTL* Reference Manual, Ver. 6.c1; Bruker Analytical X-ray Systems, Inc.: Madison, WI, 2000. (d) Sheldrick, G. M. *SHELXTL*, Ver. 6.12; Bruker AXS Inc.: Madison, WI, 2001. (e) Sheldrick, G. M. *SHELXL97*, Program for Crystal Structure Refinement; University of Göttingen: Göttingen, Germany, 1997. (f) Bradenburg, K. *Diamond*, Ver. 3.1eM; Crystal Impact GbR: Bonn, Germany, 2005. (g) Van der Sluis, P.; Spek, A. L. *Acta Crystallogr., Sect. A* **1990**, *46*, 194−201. (h) Spek, A. L. *Acta Crystallogra., Sect. A* **1990**, *46*, c34. (i) Spek, A. L. *J. Appl. Crystallogr.* **2003**, *36*, 7−13.

(14) (a) Tolis, E. I.; Helliwell, M.; Langley, S.; Raftery, J.; Winpenny, R. E. P. *Angew. Chem., Int. Ed.* **2003**, *42*, 3804−3808. (b) Tolis, E. I.; Engelhardt, L. P.; Mason, P. V.; Rajaraman, G.; Kindo, K.; Luban, M.; Matsuo, A.; Nojiri, H.; Raftery, J.; Schrçder, C.; Timco, G. A.; Tuna, F.; Wernsdorfer, W.; Winpenny, R. E. P. *Chem.—Eur. J.* **2006**, *12*, 8961−8968. (c) Yan Zhen, Z.; Winpenny, R. E. P. *Sci. China Chem.* **2012**, *55*, 910−913. (d) Khanra, S.; Konar, S.; Clearfield, A.; Helliwell, M.; McInnes, E. J. L.; Tolis, E.; Tuna, F.; Winpenny, R. E. P. *Inorg. Chem.* **2009**, *48*, 5338−5349. (e) Khanra, S.; Helliwell, M.; Tuna, F.; McInnes, E. J. L.; Winpenny, R. E. P. *Dalton Trans.* **2009**, 6166−6174. (f) Konar, S.; Bhuvanesh, N.; Clearfield, A. *J. Am. Chem. Soc.* **2006**, *128*, 9604−9605. (g) Konar, S.; Clearfield, A. *Inorg. Chem.* **2008**, *47*, 5573−5579. (h) Yao, H.-C.; Wang, J.-J.; Ma, Y.-S.; Waldmann, O.; Du, W.-X.; Song, Y.; Li, Y.-Z.; Zheng, L.-M.; Decurtins, S.; Xin, X.-Q. *Chem. Commun.* **2006**, 1745−1747. (i) Murugavel, R.; Gogoi, N.; Clérac, R. *Inorg. Chem.* **2009**, *48*, 646−651.

(15) Zavras, A.; Fry, J. A.; Beavers, C. M.; Talbo, G. H.; Richards, A. F. *CrystEngComm* **2011**, *13*, 3551−3561.

(16) Gopal, K.; Tuna, F.; Winpenny, R. E. P. *Dalton Trans.* **2011**, *40*, 12044−12047.

(17) Du, Z.-Y.; Sun, Y.-H.; Liu, Q.-Y.; Xie, Y.-R.; Wen, H.-R. *Inorg. Chem.* **2009**, *48*, 7015−7017.

(18) Chandrasekhar, V.; Goura, J.; Sañudo, E. C. *Inorg. Chem.* **2012**, *51*, 8479−8487.

(19) (a) Pasteur, L. *Ann. Chim. Phys.* **1848**, *24*, 442. (b) Amouri, H.; Gruselle, M. *Chirality in Transition Metal Chemistry: Molecules, Supramolecular Assemblies and Materials*; John Wiley & Sons Ltd: Chichester, U.K., 2008.

(20) Coxall, R. A.; Harris, S. G.; Henderson, D. K.; Parsons, S.; Tasker, P. A.; Winpenny, R. E. P. *Dalton Trans.* **2000**, 2349−2356.

(21) Liu, W.; Thorp, H. H. *Inorg. Chem.* **1993**, *32*, 4102−4105.

(22) Addison, A. W.; Rao, T. N.; Reedijk, J.; van Rijn, J.; Verschoor, G. C. *J. Chem. Soc., Dalton Trans.* **1984**, 1349−1356.